Cognitive multi-user free space optical communication testbed

Federica Aveta, Samuel Chan, Hazem Refai

Federica Aveta, Samuel Chan, Hazem H. Refai, "Cognitive multi-user free space optical communication testbed," Proc. SPIE 11678, Free-Space Laser Communications XXXIII, 1167804 (5 March 2021); doi: 10.1117/12.2575915

SPIE.

Event: SPIE LASE, 2021, Online Only

Cognitive multi-user free space optical communication testbed

Federica Aveta[a], Samuel Chan[a], Hazem H. Refai[a]
[a]Department of Electrical Engineering, University of Oklahoma, Tulsa, USA

ABSTRACT

Multi-point free space optical communication (FSOC) has been identified as a valuable and promising technology for meeting high-capacity and -density demands of future space and terrestrial communication networks. FSOC's point-to-point nature has boosted extensive research on technologies and methods that support multi-user optical networks. An FSOC system platform is essential for fully characterizing, testing, and evaluating state-of-the-art, multi-user prototypes and technologies developed by both businesses and academic communities. This paper presents an experimental FSOC testbed that demonstrates next generation FSO systems and allows cognitive, multi-point communication. These systems provide a significant improvement over those with currently hampered with single-user limitations. The FSOC testbed is multi-node, modular, and high-speed with real-time ability to test O-PHY modules and O-MAC schemes. The testbed consists of multiple, independently tunable optical transmitters and receivers that can be configured to emulate various communication scenarios (e.g., point-to-point (P2P), point-to-multipoint (P2MP), and multi-point-to-multipoint (MP2MP). At the receiver side, a cognitive controller performs real time, blind processing of received signals for identifying the number of concurrent transmissions. Accordingly, the controller drives an optical switch to route detected signals to pre-defined paths. Given that a single-user transmission is detected on multiple paths, diversity combining will be performed to improve received signal-to-noise ratio (SNR). If multiple-user transmissions are identified, signals are routed into separate high-speed photodetectors for processing. The work described below details hardware components integrated in the platform, as well as software development for the cognitive controller. Furthermore, this work provides an experimental demonstration of the testbed capabilities for single-user and multiple-user scenarios.

Keywords: Free Space Optical Communication (FSOC), Optical Wireless Communication (OWC) testbed, cognitive optics, multi-user communication.

1. INTRODUCTION

Free space optical communication (FSOC) has been proposed as a valuable technology for meeting the high-capacity and-density demands of future 5G communication resulting from spectrum shortage in existing radio frequency (RF) technology[1]. FSO offers high, unlicensed bandwidth, low power consumption, high data-rate, low-cost, and easy deployment, as well as secure and interference-immune networks[2]. FSO network implementation suffers from critical challenges (e.g., link blockage, user interference, misalignment, atmospheric turbulence, and weather effects) that can degrade system performance. Researchers have been investigating different hardware and software solutions to mitigate such technology limitations[3]. To fully characterize, test and evaluate developed prototypes and proposed technologies designed to overcome these limitations, an FSO system facility equipped with appropriate infrastructure and diagnostic equipment is essential. Several research groups in universities, private organizations, and governmental agencies have proposed and constructed testbed facilities to tackle various constraints of FSOC.

Authors in[4] presented a testbed fabricated at the Johns Hopkins University Applied Physics Laboratory designed to emulate an FSO mobile tactical network. The testbed evaluates network topology and restoration at the physical (PHY), logical link, and networking layers. Software tools were developed for network management, including the tactical edge network emulation tool (TENET)[5] and distributed adaptive pre-computed restoration (DAPR) algorithm[6]. The FSO network consisted of six nodes connected to a MEMS optical switch for dynamically configuring links between fixed nodes. Mobility was emulated in a static infrastructure. Notably, practical issues related to mobility (e.g., misalignment) that could affect the network topology reconfiguration were not addressed in this work. In Japan, the National Institute of Information and Communication Technology has been working with a terrestrial free-space optical communications network (INNOVA) testbed to implement a site diversity technique equipped with several optical ground stations[7,8]. Receiver diversity performs high-speed data transmission in future airborne- and satellite-based optical communication. A ground station network was equipped with several large aperture telescopes (e.g., 1 m) linked through a wired network and controlled remotely by an optical ground station control center. The switching mechanism in ground stations was

Free-Space Laser Communications XXXIII, edited by Hamid Hemmati,
Don M. Boroson, Proc. of SPIE Vol. 11678, 1167804 · © 2021 SPIE
CCC code: 0277-786X/21/$21 · doi: 10.1117/12.2575915

triggered by weather and channel atmospheric conditions. Environmental data collection stations were installed at several Japanese sites to collect climate data from sensors network. However, no point, acquisition, and tracking (PAT) mechanisms were considered or proposed for performing channel switching. Authors in[9,10] presented an experimental testbed to prove high-speed (e.g., >1.6 Tbps) FSO communication in an uplink GEO satellite and proposed using transmitter diversity to reach projected throughput performance. The testbed is part of the terabit throughout satellite technology (THRUST) project undertaken by the German Aerospace Center (DLR) and is composed of three main subsystems, namely communications, optomechanical, and metrology. To perform transmit diversity, dense wavelength division multiplexing (DWDM) with 40 channels in the optical C-band was proposed.

Several research groups have introduced and implemented a testbed to further characterize and study the atmospheric turbulence profile. Authors in[11] reported on the atmospheric laser optics testbed (A-LOT) located at the Army Research Laboratory (ARL) facility. A-LOT includes a 2.3 km horizontal propagating path that connects the 12m above ground laboratory building with a 73 m water tower. The laboratory site is equipped with a transceiver from the TereScope 3000 laser communication system designed to provide a communication link with the tower; a transceiver for live imagery transmission and adaptive optics; a scintillometer; and several high-speed CCD cameras for measuring intensity of scintillations. The system leverages a sensor network for continuous, real-time monitoring of atmospheric conditions. Laser-beam parameters are equipped with a scintillometer, visibility sensor, weather station, and system for providing meteorological data. Artificial smoke, fog, and rain generators were installed in the laboratory facility to simulate controllable weather conditions. A maritime lasercom test facility (LCTF) at the U.S. Naval Research Laboratory is presented in[12,13]. LCTF is characterized by 16 km one-way and 32 km round-trip links over the water. The transmitting side is located on a building 30 m above water level and equipped with an FSM that controls pointing and system alignment. On the other side, optical receivers, atmospheric diagnostic equipment, and computer control systems are positioned at approximately water level, guaranteeing a 16 km communication link and analysis of atmospheric conditions. The testbed focused exclusively on the atmospheric turbulence effects of propagating optical signals.

To the best of our knowledge, no complete testbed is able to emulate an intelligent multi-point-to-multi-point (MP2MP) communication network under different atmospheric turbulence scenarios., Notably, this paper presents an intelligent FSOC testbed that is multi-node, modular, high-speed, and real-time capable of testing optical PHY modules and multiple access control (MAC) schemes. The work detailed below describes the testbed design and the proposed cognitive algorithm for embedding intelligence in the system. Preliminary experimental results are illustrated for diverse communication scenario to highlight system capabilities and limitations. The balance of this paper is organized as follows. Section 2 describes testbed hardware and software design, and Section 3 reports experimental results. Section 4 concludes the paper and indicates possible future work.

2. TESTBED

2.1 Testbed design

A depiction of the proposed testbed is illustrated in Fig. 1. Free-space optical pathways are drawn in light blue; fiber-based optical pathways are drawn in blue; and electrical pathways are drawn in black. The testbed is composed of four independently tunable, optical transmitters that can be configured and combined to emulate various communication scenarios through the use of optical combiners, power splitters, attenuators, and phase shifters. As such, diverse user configurations can be implemented (e.g., single user on single channel, single user on multiple channels, multiple users on single channel, and multiple users or multiple channels). A picture of the OWC testbed is illustrated in Fig. 2. Each transmitting node consists of an optical laser source (i.e., λ_1= 1310 nm or λ_2 = 1550 nm operating wavelength) with variable transmitting power driven by independently configurable PRBS. Nodes are based on an intensity modulation (i.e. on-off keying [OOK]) with direct detection (IM/DD) scheme. Laser 1 includes a high-speed digital reference optical transmitter (i.e., C-band Thorlabs MX10B) with embedded optical attenuator for tuning transmitted power. Remaining lasers are composed of optical module transceivers (SFP, 1310/1550 nm wavelengths) that are independently driven via Hitech Global SMA to SFP conversion modules and an external variable optical attenuator (Thorlabs VOA50-FC) for varying transmitted power. PRBSs are generated with two independent, dual-channel pulse/arbitrary waveform generators, namely SIGLENT's SDG6032X. Each channel can be independently configured to generate the desired PRBS bit-rate, amplitude, and length. Transmitted signals can be combined using optical combiners and power splitters with various input-output configurations (e.g., 4x1, 2x1, 2x2, and the like) to cover several configuration scenarios. Figs. 1 and 2 illustrate a

configuration that uses 2x1 optical combiners for combining two users into one mixed signal. Two pairs of collimators with 1550 nm and 1310 nm wavelength-dependent lenses were used to propagate combined signals through a free space turbulent and/or non-turbulent channel. Atmospheric turbulence can be generated and evaluated using the turbulence box detailed in[14]. Received optical signals are collected by two 1x2 MEMS optical switches, namely Thorlabs OSW12-1310E. The design and configuration of the two optical switches make them function as a single 2x4 optical switch, as illustrated in Fig. 3. If received optical signals IN1 and IN2 are copies of the same signal (i.e., single-user), the optical switch will route input signals to OUT1_2 and OUT2_2 (i.e., State2) to be summed with the optical combiner and increase signals SNR and, therefore, signal quality[15]. Signals are then directed to a photodetector for signal processing. Given that IN1 and IN2 are two different signals (e.g., multiple-users or different single-users), the optical switch will guide signals directly through OUT1_1 and OUT2_1 (i.e., State1) to the photodetectors for signal decoding. Three 5-GHz bandwidth InGaAs photodetectors, namely Thorlabs DET08CFC, were used for optical-to-electrical conversion. Photodetector outputs were connected to WavePro 254HD-MS oscilloscope with a 20 GSample/s sampling rate for data collection and visualization.

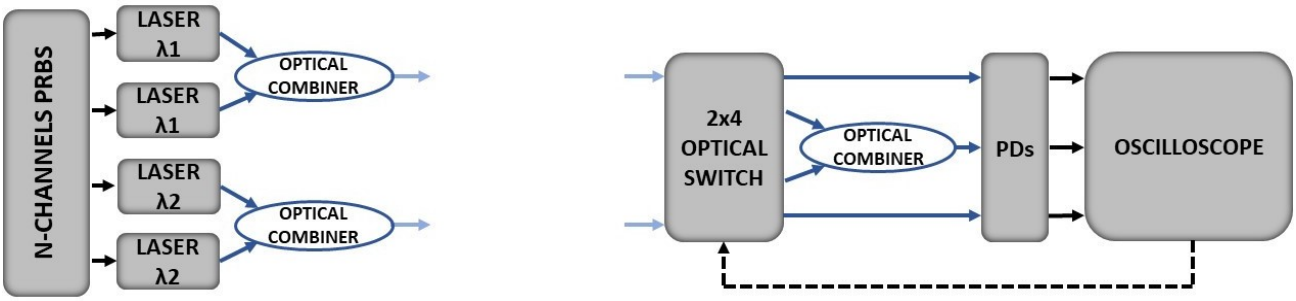

Figure 1: OWC testbed depiction.

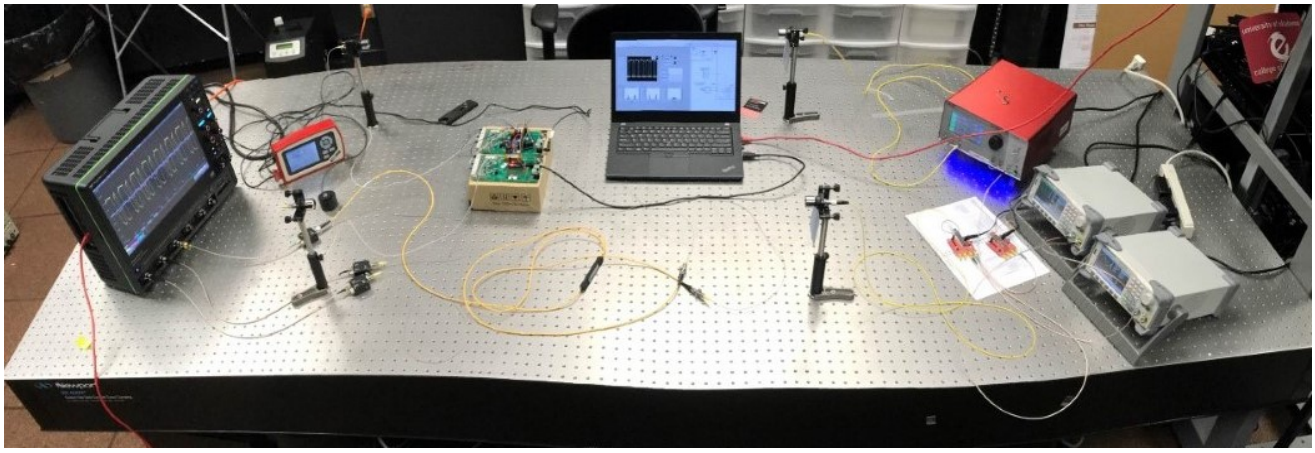

Figure 2: OWC testbed.

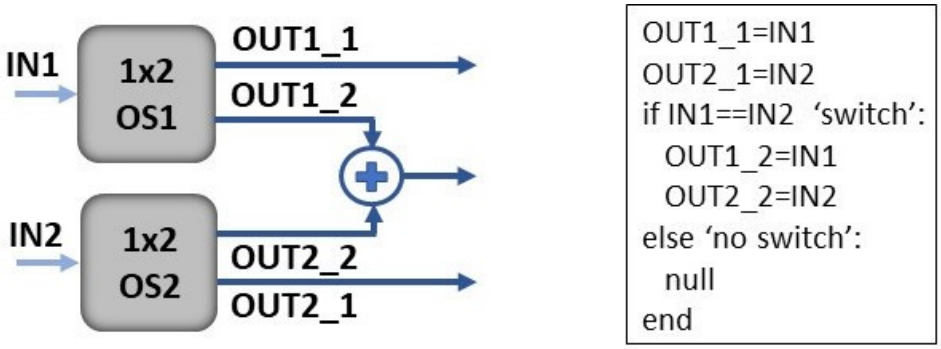

Figure 3: Optical switch working principle.

2.2 Cognitive controller

The switching mechanism is driven by a cognitive controller that detects and compares received signals at inputs IN1 and IN2. The controller observes received signals, compares them using an intelligent algorithm, and drives the optical switch accordingly. Thus, the controller determines if single or multiple users are transmitting into the receiver and if the same user is received at multiple nodes (i.e., IN1 and IN2). Fig. 4 provides a system flowchart that describes the proposed algorithm developed in LabVIEW. The optical switch is controlled by the on-board logic board and triggered by a transistor–transistor logic (TTL) signal. First, the system synchronizes both switches, setting them to State1 (i.e., OUT1_1 and OUT2_1), which enables State1 loop to commence. Next, the oscilloscope samples each corresponding channel, wherein each input (i.e., IN1 and IN2) has its own oscilloscope channel on State1. Then, the number of received users is calculated using the methodology developed in[16]. If only a single or a fixed number of users is detected in both channels, similarity between channels (e.g., cross-correlation and cosine similarity) will be computed to evaluate if signals received at IN1 and IN2 are signals from ~~of~~ the same-user signal or if signals are coming from independent users. Given high similarity between received signals, the channels will be switched to State2 (i.e., OUT1_2 and OUT2_2), wherein the switch outputs will be combined via an optical combiner to increase signal strength. In State2, the system will wait for a period—two seconds in this setup—to protect the switch from high speed and frequent switching, and then number of users in State2 will be re-calculated. Given that this number has increased, the system will switch back to the initial State1; otherwise, the system will continue in a State2 loop.

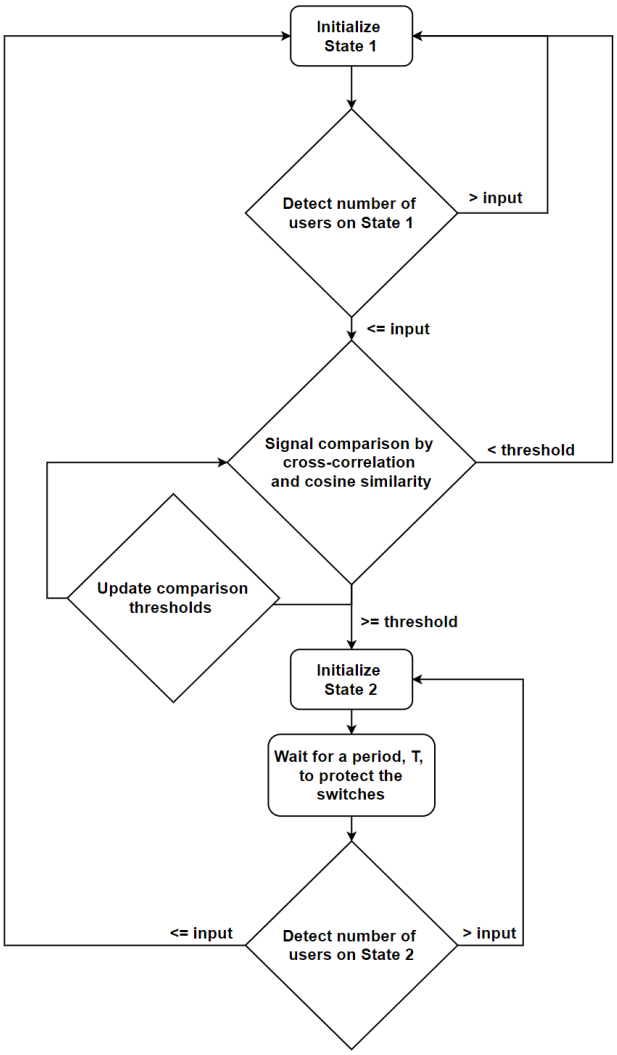

Figure 4. System flowchart.

2.2.1 Similarity measure

a) Cosine similarity

Cosine similarity between two vectors A and B is defined as follows:

$$\cos(\theta) = \frac{A \cdot B}{|A||B|}$$

b) Cross-correlation

Cross-correlation between two vectors A and B is defined as follows:

$$\max(R_{AB}) = \max\left(E[AB^T]\right)$$

c) Threshold determination

Threshold determination was necessary for identifying the optimum value for triggering the switch mechanism from State1 to State2 and vice-versa. The system initializes State1, wherein each input signal has its own oscilloscope channel. Given that signals are similar (i.e. similarity coefficients greater than threshold), they will be combined, and the system will switch to State2. Ideally, a similarity close to 1 should be measured if IN1 and IN2 receive copies of the same signal; however, given that two identical signals might undergo different channel conditions, a similarity value less than 1 is realistically expected. Analysis was conducted by varying the threshold value from 0 to 1 with 0.1 steps and two identical synchronized users. Error rate was calculated as the number of times the system did not switch from State1 to State2, given that similarity measures were confirmed above threshold over the total number of trials.

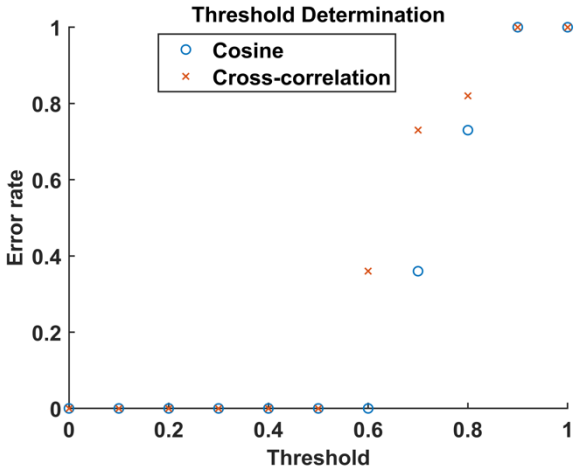

Figure 5. Threshold analysis.

Fig. 5 shows that an error rate greater than zero was measured at thresholds greater than 0.5 for cross-correlation and 0.6 for cosine similarity. This means that two identical users undergoing different channel conditions will result in cross-correlation greater than 0.5 and cosine similarity greater than 0.6. Accordingly, these values were selected as optimum threshold values; each time the system measures similarity coefficients greater than these optimum values, a switch from State1 to State2 should be performed.

2.2.2 Results

Fig. 6 shows the LabVIEW graphical user interface (GUI) of the algorithm running on two channels with identical synchronized signals operating on State1. The top left figure shows the real-time waveforms of the three channels; the white and blue waveforms correspond to OUT1_1 and OUT2_1, and the green waveform to the combiner output. Given the system is in State1, no signal is routed to the combiner. Three real-time histograms illustrate the normalized frequencies corresponding to the real-time received signals' amplitude illustrated in the real-time waveform channels. The three LED indicators inform as to whether corresponding similarities based on results are above threshold. The AND indicator informs if both similarities are above threshold. When the indicator is lit, the system is ready to switch to State2. The fields "#peaks @ ch" indicates the number of peaks detected and consequently the number of users monitored in real time on each

channel. LEDs on the right indicate if the number of users is greater than the sum of the users on each channel in the previous state. As mentioned before, when this occurs in State2, the system will switch back to State1.

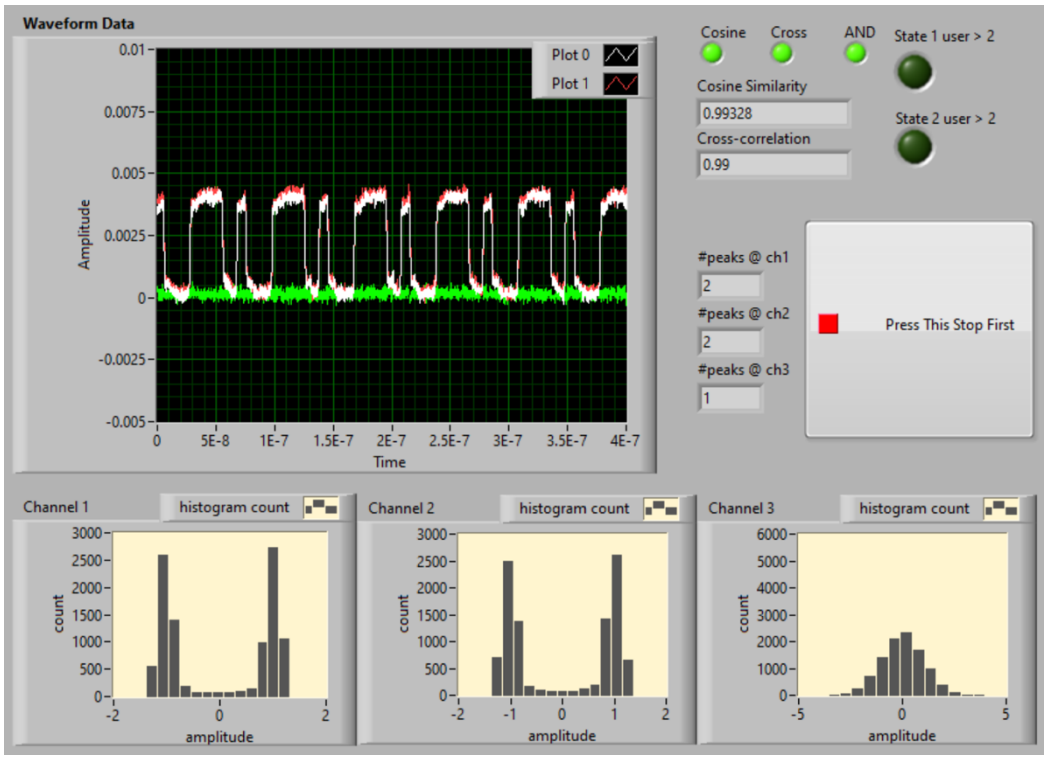

Figure 6. GUI.

To validate the implemented algorithm for controlling the switching mechanism, diverse user configurations were tested and are shown in Figs. 7 and 8. The system was tested with single, dual, and triple users combined via an optical combiner before passing through a channel. Fig. 7 shows the histogram of the real-time received signal in diverse State configurations. Fig. 7a) illustrates the case of two identical synchronized users when the system is in State1; Fig. 7b) illustrates the same user scenario after the switching from State1 to State2. Finally, Fig. 7c) depicts a scenario with one user at IN1 and two users at IN2; hence, the system does not switch and remains in State1. Results demonstrate that histograms showed the correct number of users, according to the number of transmitting users. To prove the effectiveness of the determined threshold, real-time received signals are illustrated to relate the received waveforms to the similarity coefficients. Fig. 8a) illustrates two identical received signals in which both cosine and cross-correlation were above thresholds; all green LEDs (i.e., three in total) were on, meaning that the system correctly switched from State1 to State2. Fig. 8b) shows two identical asynchronized users, indicating cross-correlation was above threshold while cosine similarity was below. Since the AND condition was not satisfied, the system remained in State1. Cases with asynchronized users should be studied as future work.

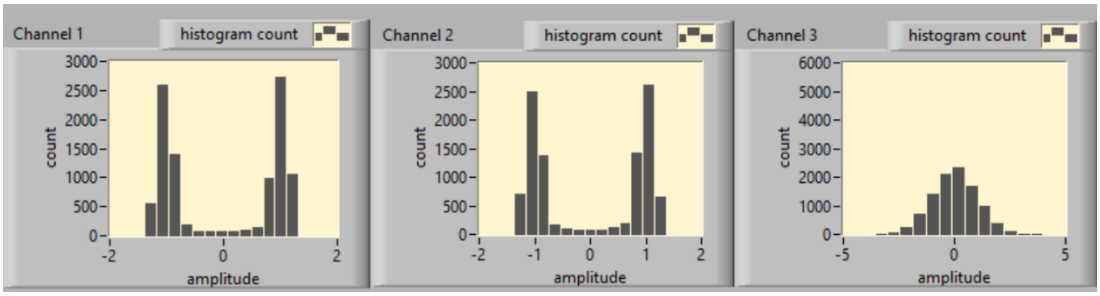

a)

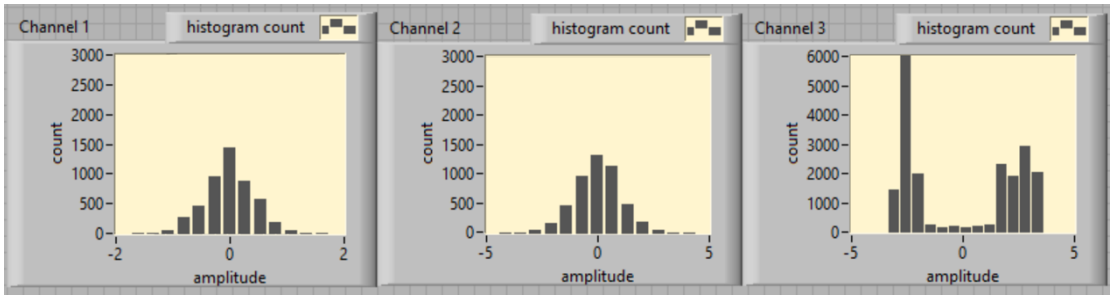

b)

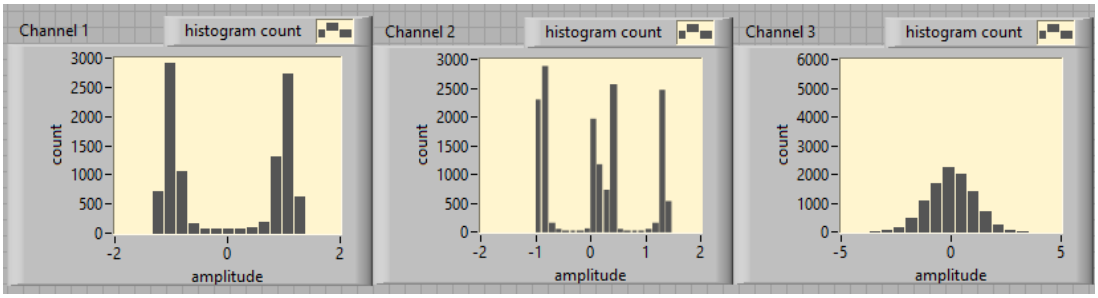

c)

Figure 7. Histograms of received signals amplitude: a) two identical users with switch in State1; b) two identical users with switch in State2; c) three different users with switch in State1.

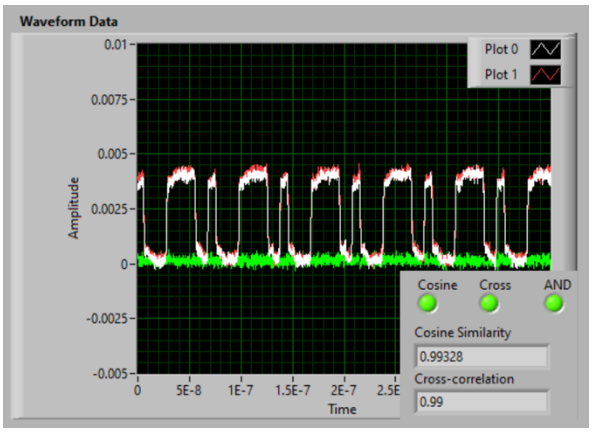

a)

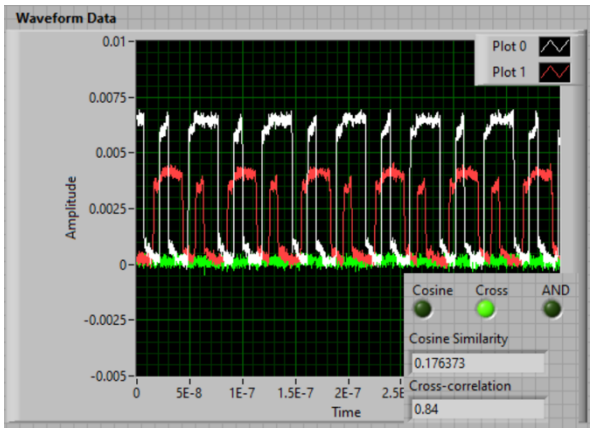

b)

Figure 8. Real-time received signals amplitude: a) two identical users; b) two identical asynchronized users.

3. MEASUREMENTS

To prove and validate testbed capabilities and to highlight testbed limitations, several experiments were conducted. Preliminary results of BER, attenuation, insertion losses, and multiple-user configuration analysis were reported.

3.1 BER Analysis

To evaluate high-speed, single-user communication capabilities, BER measurements were collected for varying transmitted power and data rate, as illustrated in Fig. 9. User 1 was selected for the analysis, and BER measurements were collected using the BertScope analyzer, SyntheSys Research BSA12500A. Transmitted power was varied from -4 dBm to 5 dBm. BER versus power is shown in Fig. 9a); low BER was obtained for transmitted power greater than 0 dBm. Fig. 9b) shows how BER increased with data rate within the range 1 Gbps to 5 Gbps. Notably, BER values greater than 10^{-3}

were obtained due to limited photodetector bandwidth. Upgrading the photodetectors would allow single-user communication with speeds greater than 10 Gbps.

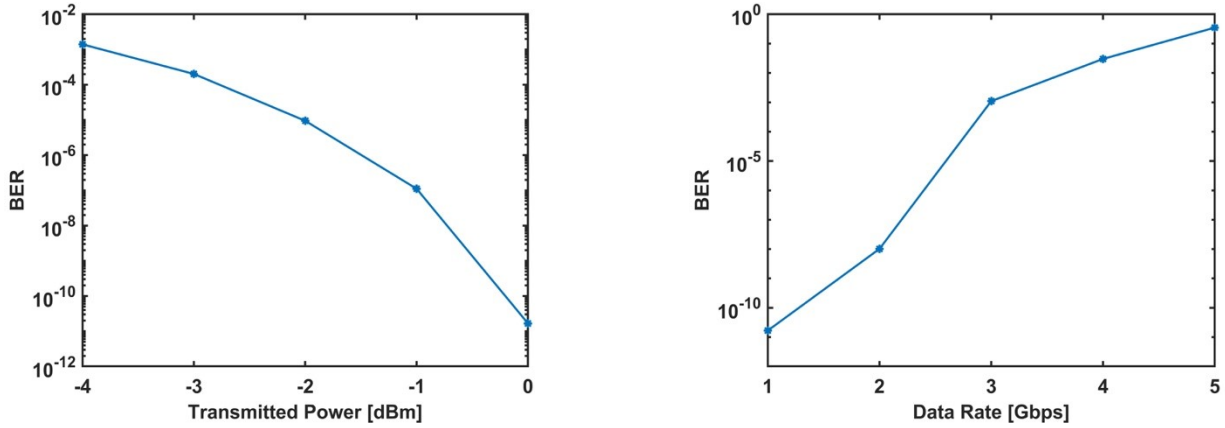

a) b)

Figure 9. BER versus: a) transmitted power; b) data rate.

3.2 Loss Insertion

Employed techniques for estimating number of transmitting users is a power-based methodology. These techniques use received signal amplitude as a distinct feature for detecting and decoding simultaneously transmitting users. As such, power analysis in terms of attenuation and insertion losses is crucial for testing proposed techniques. Received optical power was measured in various sections along the optical link using the optical spectrum analyzer Advantest Q8384. In particular, optical power figures before the optical switch, after the switch, and after the optical combiner were collected. Transmitted optical power of user 1 was varied from -2 dBm to 5 dBm with 1 Gbps data rate.

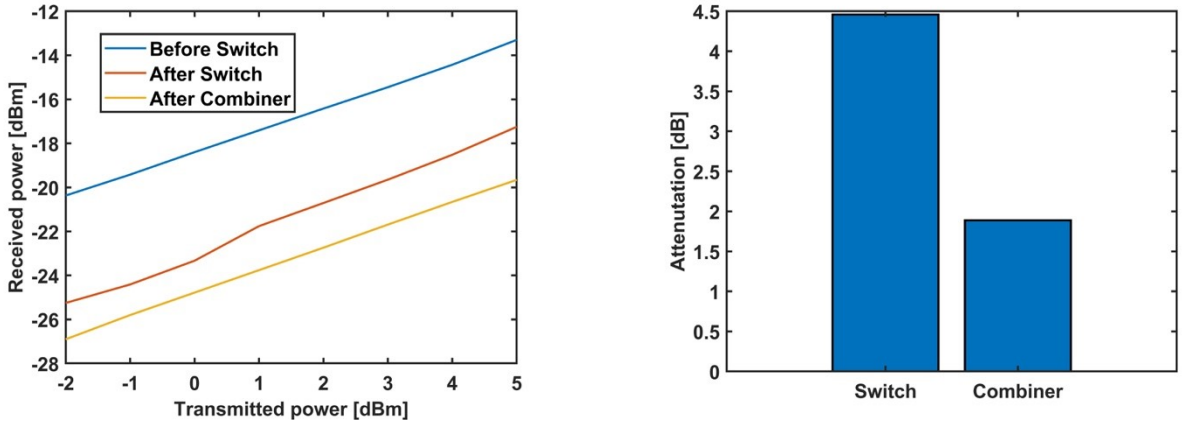

a) b)

Figure 10: a) loss insertion; b) total attenuation.

Fig. 10a) shows received optical power [dBm] versus transmitted optical power [dBm] before and after the optical switch, as well as after the optical combiner. Received optical power decreased linearly with reducing transmitted power for all three studied sections. Fig. 10b) illustrates average total attenuation [dB] introduced by the optical switches (4.46 dB) and by the optical combiner (1.88 dB). Total average insertion loss at the receiving side of 6.34 dB was obtained. Total attenuation resulted from device insertion losses and fiber connection coupling losses. To decrease losses, it is suggested that customized devices and/or multi-mode devices could be adopted, which would also result in additional coupling power.

3.3 Multi-user configuration

The transmitting side of the OWC testbed consists of four independently tunable users that can be configured to emulate various communication scenarios. Data in the time domain and frequency domain can be displayed and collected for further analysis. Fig. 11 shows possible experimental scenarios in which transmitted power and data rate for each user were 2.87 dBm and 50 Mbps for user 1; 1 dBm and 250 Mbps for user 2; -2.81 dBm and 150 Mbps for user 3; and -3.98 dBm and 100 Mbps for user 4. Single user on single channel, single user on multiple channels (e.g., two), multiple users (e.g., four) on single channel, and multiple users (e.g., three) on multiple channels (e.g., two) are illustrated in 11 a), b), c) and d) respectively.

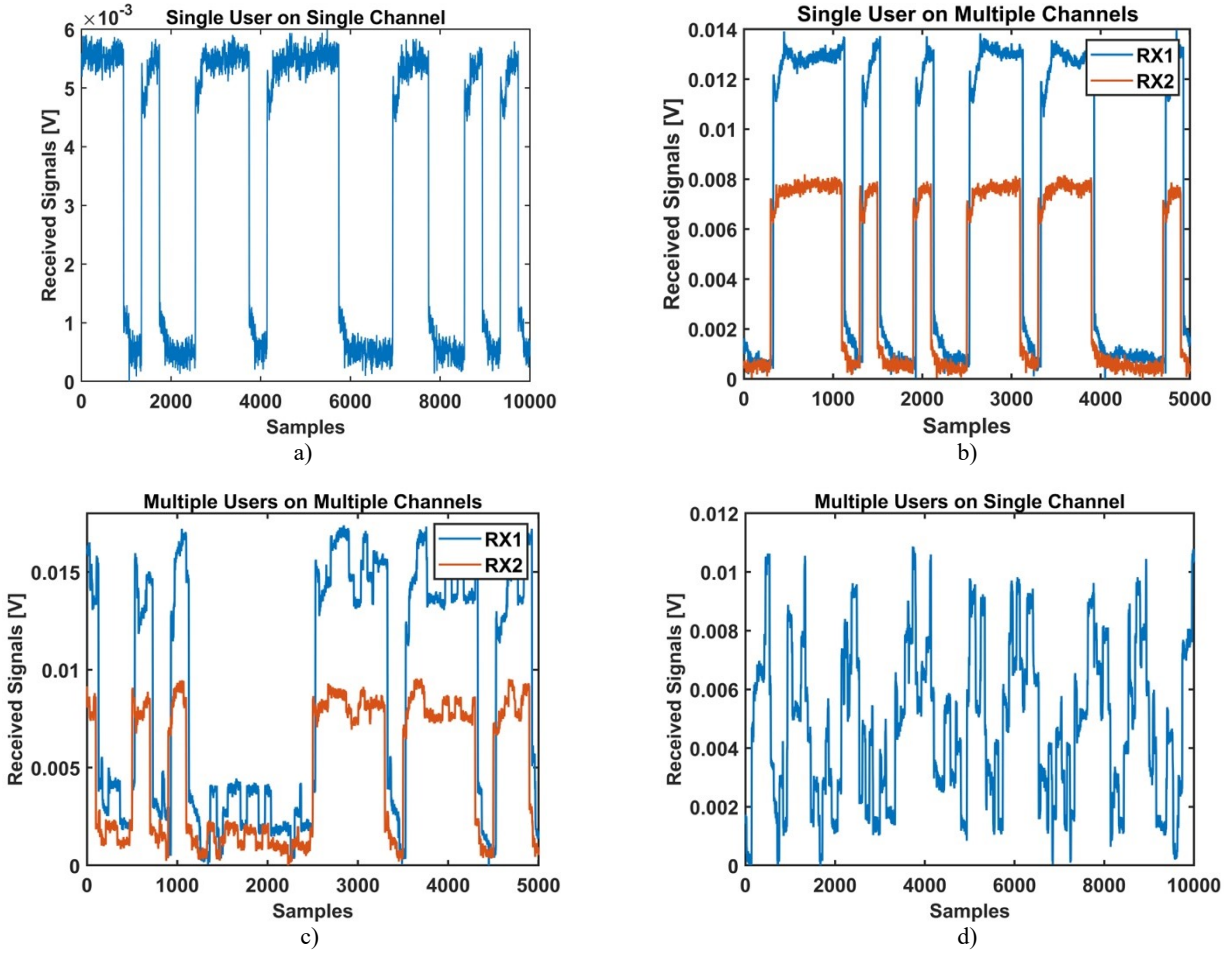

Figure 11. Communication scenarios: a) Single user on single channel; b) Single user on multiple channels; c) Multiple users on single channel; d) Multiple users on multiple channels.

CONCLUSION AND FUTURE WORK

The design, implementation, and testing of an OWC testbed was conducted to emulate cognitive, multi-user communication scenarios and to test and evaluate intelligent algorithms and multi-point communication technologies. The testbed consists of multiple, independently tunable optical transmitters that can be configured to emulate various communication scenarios (e.g., point-to-point, point-to-multipoint, multipoint-to-multipoint). At the receiver side, an optical switch, driven by a cognitive controller, was adopted to route detected signals to pre-defined pathways for signal processing. Testbed and cognitive controller capabilities and effectiveness for single-user and multiple-user scenarios were demonstrated. Besides providing preliminary results for experiments carried out for this work, the OWC testbed represents a research and testing platform that could be exploited by both research and commercial entities for testing and validating a wide spectrum of ideas and applications. The platform targets a variety of application scenarios for testing several FSOC systems for space, aerial, and terrestrial communication links. Examples of system capabilities that can be tested with the

actual testbed include time-domain and frequency-domain analysis, real-time and offline analysis, point-to-point and multipoint-to-multipoint analysis, omni-directional receiver, atmospheric turbulence, noise effects, diversity combining, and BER analysis. Future work will include upgrading the current software and hardware testbed design to extend the listed capabilities. Additional scenarios and applications could be emulated and evaluated, including higher number of users, multi-level modulation format, user mobility, and pointing errors.

REFERENCES

[1] Chowdhury, M. Z., Hossan, M. T., Islam, A. and Jang, Y. M., "A comparative survey of optical wireless technologies: architectures and applications," IEEE Access 6, 9819–9840 (2018).

[2] Khalighi, M. A. and Uysal, M., "Survey on Free Space Optical Communication: A Communication Theory Perspective," IEEE Commun. Surv. Tutorials 16(4), 2231–2258 (2014).

[3] Kaushal, H. and Kaddoum, G., "Optical communication in space: Challenges and mitigation techniques," IEEE Commun. Surv. Tutorials 19(1), 57–96 (2017).

[4] Turner, W. M., Tebben, D. J., Madsen, J. R. and Dwivedi, A., "A testbed to emulate next-generation directional RF and free-space optical tactical networks," Testbeds Res. Infrastructures Dev. Networks Communities Work. 2009. TridentCom 2009. 5th Int. Conf., 1–5, IEEE (2009).

[5] Tebben, D., Dwivedi, A., Madsen, J., Turner, W., Garretson, J. and Frey, T., "Tenet (tactical edge network emulation tool): A tool for connectivity analysis for tactical scenario," Mil. Commun. Conf. 2008. MILCOM 2008. IEEE, 1–7, IEEE (2008).

[6] Harshavardhana, P., Tebben, D. J., Dwivedi, A. and Hammons, A. R., "DAPR (Distributed adaptive precomputed restoration): An Algorithm for Assured availability Directional RF and FSO MANET," Mil. Commun. Conf. 2007. MILCOM 2007. IEEE, 1–6, IEEE (2007).

[7] Toyoshima, M., Munemasa, Y., Takenaka, H., Takayama, Y., Koyama, Y., Kunimori, H., Kubooka, T., Suzuki, K., Yamamoto, S. and Taira, S., "Terrestrial Free-Space Optical Communications Network Testbed: INNOVA," Proc. ICSOS, S2-4 (2014).

[8] Toyoshima, M., Munemasa, Y., Takenaka, H., Takayama, Y., Koyama, Y., Kunimori, H., Kubooka, T., Suzuki, K., Yamamoto, S. and Taira, S., "Introduction of a terrestrial free-space optical communications network facility: IN-orbit and Networked Optical ground stations experimental Verification Advanced testbed (INNOVA)," Free. Laser Commun. Atmos. Propag. XXVI 8971, 89710R, International Society for Optics and Photonics (2014).

[9] Giggenbach, D., Poliak, J., Mata-Calvo, R., Fuchs, C., Perlot, N., Freund, R. and Richter, T., "Preliminary results of Terabit-per-second long-range free-space optical transmission Experiment THRUST," Unmanned/Unattended Sensors Sens. Networks XI; Adv. Free. Opt. Commun. Tech. Appl. 9647, 96470H, International Society for Optics and Photonics (2015).

[10] Poliak, J., Giggenbach, D., Moll, F., Rein, F., Fuchs, C. and Calvo, R. M., "Terabit-throughput GEO satellite optical feeder link testbed," Telecommun. (ConTEL), 2015 13th Int. Conf., 1–5, IEEE (2015).

[11] Vorontsov, M. A., Carhart, G. W., Banta, M., Weyrauch, T., Gowens, J. and Carrano, J. C., "Atmospheric Laser Optics Testbed (A_LOT): Atmospheric propagation characterization, beam control, and imaging results," Adv. Wavefront Control Methods, Devices, Appl. 5162, 37–49, International Society for Optics and Photonics (2003).

[12] Burris, H. R., Moore, C. I., Swingen, L. A., Vilcheck, M. J., Tulchinsky, D. A., Mahon, R., Wasiczko, L. M., Stell, M. F., Davis, M. A. and Moore, S. W., "Latest results from the 32 km maritime lasercom link at the Naval Research Laboratory, Chesapeake Bay Lasercom Test Facility," Atmos. Propag. II 5793, 209–220, International Society for Optics and Photonics (2005).

[13] Moore, C. I., Burris, H. R., Rabinovich, W. S., Wasiczko, L., Swingen, L. A., Mahon, R., Stell, M. F., Gilbreath, G. C. and Scharpf, W. J., "Overview of NRL's maritime laser communication test facility," Free. Laser Commun. V 5892, 589206, International Society for Optics and Photonics (2005).

[14] Aveta, F., Refai, H. H. and LoPresti, P., "Multiple access technique in a high-speed free-space optical communication link: independent component analysis," Opt. Eng. 58(3), 36111 (2019).

[15] Moradi, H., Refai, H. H., LoPresti, P. G. and Atiquzzaman, M., "Diversity combining for mobile FSO nodes in SIMO setup," Wirel. Commun. Mob. Comput. Conf. (IWCMC), 2011 7th Int., 2243–2248, IEEE (2011).

[16] Aveta, F., Refai, H. H. and LoPresti, P., "Cognitive Multi-Point Free Space Optical Communication: Real-Time Users Discovery using Unsupervised Machine Learning," IEEE Access, 1 (2020).